Nanoscale

Accepted Manuscript

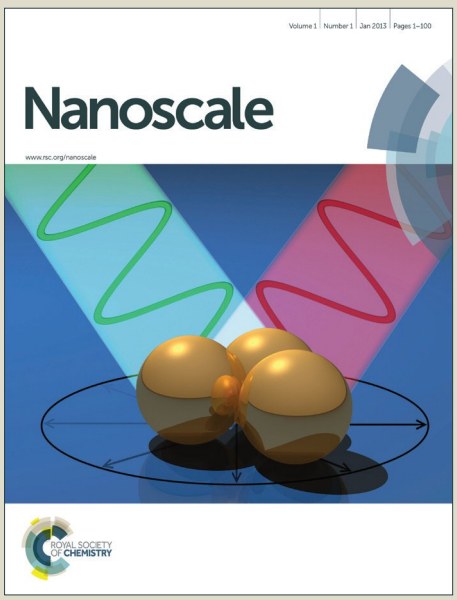

ROYAL SOCIETY OF CHEMISTRY

www.rsc.org/nanoscale

Cite this: DOI: 10.1039/c0xx00000x

www.rsc.org/xxxxxx

ARTICLE TYPE

Ultrasensitive SERS detection of trinitrotoluene through capillarity-constructed reversible hot spots based on ZnO-Ag nanorods hybrids

Xuan He,*[a] Hui Wang,[a] Zhongbo Li,*[b] Dong Chen,[a] Jiahui Liu,[a] and Qi Zhang*[a]

Received (in XXX, XXX) Xth XXXXXXXXX 20XX, Accepted Xth XXXXXXXXX 20XX

DOI: 10.1039/b000000x

A simple and efficient self-approach strategy was used to applied ultrasensitive and self-revive ZnO-Ag hybrids surface-enhanced Raman scattering (SERS) sensors for the highly sensitive and selective detection of explosive TNT in both solution and vapour conditions. The performance of ultrasensitive sensing was from abundant Raman hot spots, which were spontaneously formed in a reversible way by the self-approaching of flexible ZnO-Ag hybrid nanorods driven through the capillary force of solvent evaporation. And the enhancement effect was repeatedly renewable by the reconstruction of molecular bridges and could selectively detect TNT with a lower limit of 4×10^{-14} M. Meanwhile, the TNT vapor was also collected under this sensor, once the ZnO-Ag NRs hybrids substrate was dipped of TNT, as been marked, this substrate could inform the existence of TNT even in 5 detection cycle through capillarity-constructed reversible hot spots approach. Compared with other pure Ag-based SERS sensor, this ZnO-Ag hybrids SERS sensor could rapidly self-revive SERS-activity by simple UV light irradiation and keep stable SERS sensitivity within one month when used for TNT detection. The stable and ultrasensitivity SERS substrate demonstrates a new route to eliminate the oxidized inactive problem of traditional Ag-based SERS substrates and suggests promising applications of such hybrids as real-time online sensors for explosives detection.

Introduction

Since the discovery that Raman signals could be enhanced at a rough silver electrode, surface-enhanced Raman scattering (SERS) has been a subject of interest in research for both the understanding of the enhancement mechanism and the chemosensing purpose.[1] Many studies have demonstrated that nanogaps between metal nanostructures are required to generate the "hot spots" typically associated with high SERS activity.[2] But the nanoscaled control on the interspace between two nano-building-blocks of the SERS-substrate has to face the problems with a structural reproducibility, complex processes and high cost.[3] A recent review by Liz-Marz´an and Polavarapu provided a detailed overview on a kind of flexible substrates for nanoplasmonic sensing which may provide a new prospect to overcome these problems.[4] These substrates often construct "hot spots" by self-conglutination of nanorods to trap molecules among nanorods by utilizing electronic,[5] ferroelectric,[6] thermal[7] or mechanical strain[8] effects. But in most effects the constructed "hot spots" in SERS-active nanostructures is not reversible, making the sensor usable only once. Moreover, it is still an intriguing challenge to create reversible hot spots and to trap target molecules for practical plasmonic sensing purposes.

Recently, a few brilliant reports indicate that the silver (Ag) nanotube or nanorod arrays could construct reversible Raman hot spots through the capillary force of solvent evaporation strategy with outstanding enhancement ability.[9] Unfortunately, Ag nanostructures are oxidized easily in air, resulting in a loss of the hot spots and inactivation of the SERS substrates. In addition to the reversible ultrahigh activity of SERS substrates, the stability of SERS substrates has been a major concern from the viewpoint of practical applications.[10] Nowadays, the hybrid nanostructures, such as ZnO/Ag, TiO_2/Ag, have attracted considerable attention because of their unique shape-, composition-dependent properties and multiple functionalities which are rarely achievable in single-component nanostructures.[3d, 11] It was very hopeful to solve the stability problem of Ag-based SERS substrate by the development of functional Ag-hybrid composite nanostructures as SERS substrates.[12] And the design of the stable Ag-hybrid substrate which could create reversible hot spots by capillary force effect would be promoted to apply SERS practical detection.

Refer to the real SERS application, as Raman spectrum rooting from vibrations in the chemical bonds of the analyte, any chemical species can in theory be analyzed. For this reason SERS has shown great potential of becoming a versatile analytical tool for both chemical and biochemical sensors in liquid and gas phases.[13] As such, SERS has been named as a very promising method for explosives sensing with fast analysis speed and high sensitivity being the main advantages.[14] Among all explosives,

Cite this: DOI: 10.1039/c0xx00000x

www.rsc.org/xxxxxx

ARTICLE TYPE

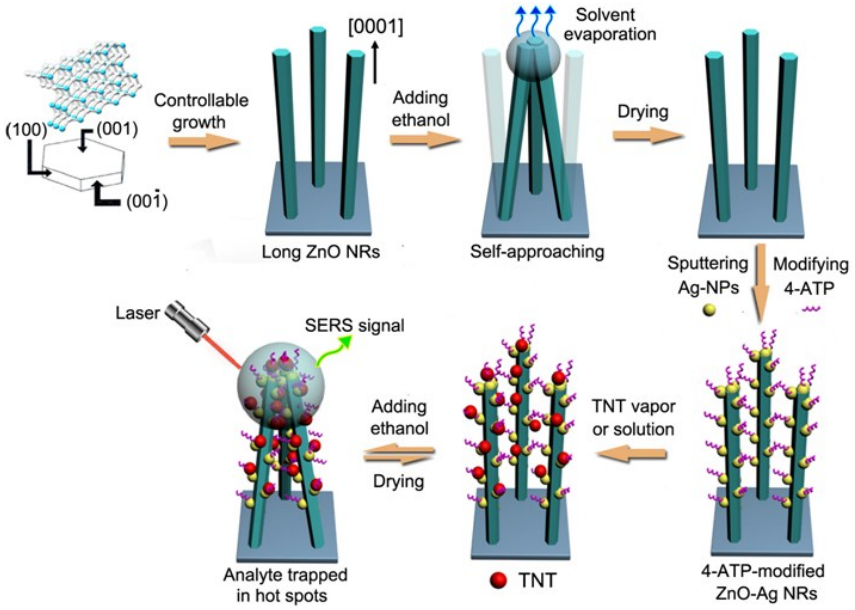

Scheme 1 schematic image of self-approaching of the NRs driven by the capillary force of solvent evaporation.

detection of illegally transported explosive materials such as 2,4,6-trinitrotoluene (TNT) is very important for various disciplines, including humanitarian demining, remediation of explosives waste sites, homeland security, and forensic applications.[15, 16] Many reports have demonstrated that SERS substrates based on the hybrid nanostructures can be repeatedly used to detect TNT.[17, 18] However, such impressive SERS face the problems with stability and reproducibility of Raman signal.

Driven by the need, in this paper, we reported for the first time the development of large-scale nanorod-shaped ZnO-Ag hybrids SERS substrates for the highly sensitive, selective, and stable detection of explosive TNT with a lower limit of 4×10^{-14} M. As shown in scheme 1, through the directional growth method designing, we could obtain vertical ZnO nanorods (NRs) with [0001] growth direction. These long ZnO NRs showed excellent flexible and could be much easier to self-approach by external effect, e.g. capillarity. Next, Ag nanoparticles (NPs) were decorated onto the surface of the ZnO NRs to fabricate ZnO-Ag hybirds as SERS substrate. Thus, high density hot spots could be formed in a reversible way via the self-approaching of ZnO-Ag NRs driven through the capillary force of solvent evaporation. Once the TNT molecules were captured via the formation of charge-transfer p, p'-dimercaptoazobenzene (DMAB)-TNT-DMAB bridge on the flexible ZnO-Ag NR array hybrids and trapped in hot spots, high enhancement Raman intensity could be achieved. Vapor of TNT was also collected under this 4-ATP-modified SERS substrate, then repeating the addition of ethanol four times and detection for five cycles with the parallel Raman intensity of 4-ATP. Cycle experiments showed that, as being marked, TNT could be persistently detected using the hot spots created through the way of solvent evaporation inspired. What's important, compared with other single-component Ag-based SERS sensor, this ZnO-Ag hybrids SERS sensor could rapidly revive the hot spots of the SERS-inactive by simple UV light irradiation and keep stable SERS-active ability within one month. The application of this stable and ultrasensitive SERS substrate would be essential for practical explosives identification and monitoring.

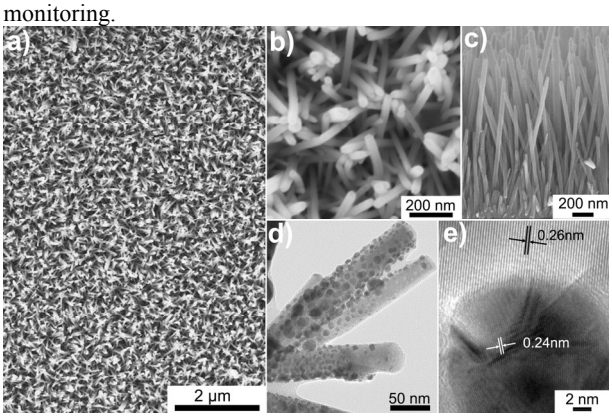

Figure 1 (a) SEM image of ZnO NRs; (b) the enlarged FE-SEM image of ZnO NRs; (c) the side view FE-SEM image of ZnO NRs; (d) TEM image of as-presented ZnO-Ag samples; (e) HRTEM images of as-presented ZnO-Ag samples of (d).

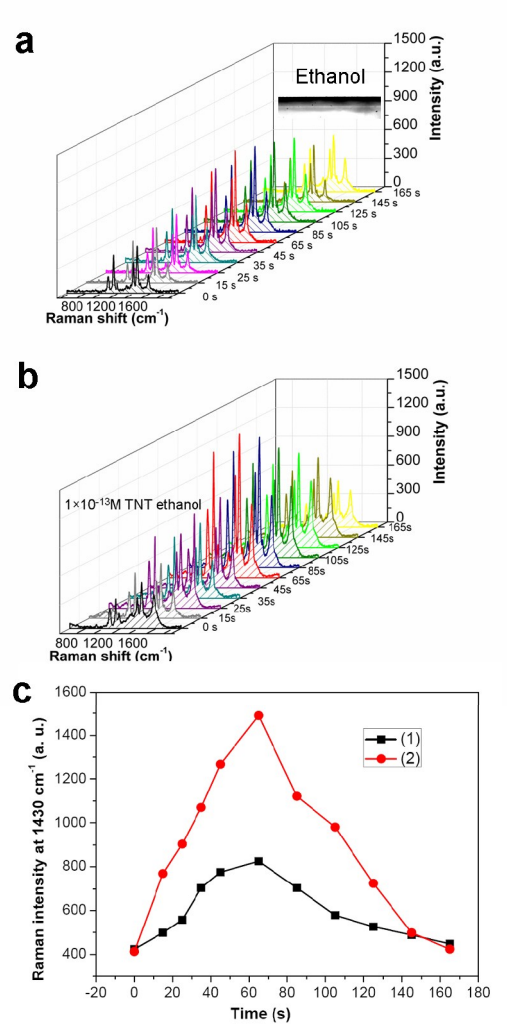

Figure 2 (a) The time-resolved Raman spectra of 4-ATP at the interval of time after dropping 5 μL ethanol, The insets in parts (a) was the photographs of ethanol droplets on the substrate; (b) 1×10^{-13} M TNT alcoholic solution on the 4-ATP modified ZnO-Ag hybrid NR arrays; (c) Line (1): The temporal evolution of corresponding Raman intensity at 1430 cm^{-1} of (a); Line (2): The temporal evolution of corresponding Raman intensity at 1430 cm^{-1} of (b).

Results and discussion

The as-prepared ZnO NRs on the substrate with different length via the simple hydrothermal method[19] was shown in supporting information (Figure 1 and S1) and characterized by field-emission scanning electron microscopy (FE-SEM). Side-view SEM images revealed that the average length of ZnO NRs was ~550nm, 960nm and 1.5μm with the reaction time 3h, 8h and 12h, respectively (1.5 μm length ZnO NRs see Figure 1(a), (b), (c) and other length ZnO NRs see Figures S1 in the Supporting Information). Moreover, the transmission electron microscopy (TEM) images further confirmed that the hybrid ZnO NRs was ~35 nm in diameter (Figure 1d). Ion sputtering was then performed to assemble Ag NPs onto the ZnO NRs with different deposition time (4 min, 10 min, 16 min, and 26 min Figure S2). High-resolution TEM (HR-TEM) images (Figure 1e) displayed clear lattice fringes of ZnO and Ag and revealed the single-crystalline nature of ZnO. Among them, the measured lattice spacing was about 0.26 nm, which corresponded to the (0002) lattice plane of wurtzite ZnO,[20] and the lattice spacing of 0.24 nm matched with the fcc Ag (111) plane, which well agreed with the XRD results (Figure S3-S4).

For evaluating the SERS effect of ZnO-Ag hybrids, the ZnO NRs with different length sputtered Ag nanoparticles with different durations were performed. Raman measurements demonstrated that 1.5 μm length ZnO nanorod arrays with 16 min Ag-sputtering showed the highest SERS activity (Figure S5). When 1×10^{-14} M R6G ethanol was directly added onto the hybrid arrays with the length of 1.5 μm, the Raman signals of R6G could clearly be detected after ~65 s (Figure S6-S8). The SERS enhancement factors (EF) for R6G on the ZnO-Ag NRs could be calculated according to the equation $EF=(I_{SERS}/I_{bulk})(N_{bulk}/N_{surface})$, where I_{SERS} and I_{bulk} were the peak intensities of 10^{-11} M R6G on the ZnO-Ag NRs substrate and 1×10^{-3} M R6G on a silicon substrate at 611cm^{-1}, respectively. N_{SERS} and N_{bulk} were the number of R6G molecules excited by the laser beam on the ZnO-Ag NRs hybrids substrate and Si substrate, respectively. And the SERS enhancement factors (EF) for R6G on the ZnO-Ag NRs could be calculated about 4.3×10^{8} after ~65s (see Supporting information Figure S6-S8).[21] This huge enhancement was due to the formation of Raman hot spot through the self-approaching of flexible ZnO-Ag NRs resulting from capillary force of solvent evaporation (scheme 1). Correspondingly, other hybrids array with length 960 nm and 550 nm exhibited much lower even no enhancement under the same condition (Figure S9-S10). It was clearly indicated that the longer ZnO NRs benefited the self-approaching and then the formation of much more Raman hot spots with the help of the capillary force of solvent evaporation due to the better flexibility.

Subsequently, different solvents were used for observation of the capillary force of solvent evaporation. Ethanol, water, acetone, methyl alcohol, isopropanol and ethyl acetate were chosen as the solvents. First, the ZnO-Ag NRs hybrids were further modified with 4-ATP through the formation of Ag-S bonds by immersing the hybrids in very dilute 4-ATP alcoholic solution (1×10^{-9} M). The Raman signal of 4-ATP molecules was very faint due to an extremely low number of molecules at these dry arrays. If a droplet of 5 μL ethanol was added onto the identical NR arrays, ethanol could completely permeate into the interspaces of the top-closed NRs (inset of Figure 2a) and the Raman spectra were recorded as shown in Figure 2a. Interestingly, with the evaporation of ethanol, the enhanced Raman signals of 4-ATP gradually appeared after ~25 s and achieved the strongest value at ~65 s (Figure 2a). Following, the enhanced signals kept the equivalent intensity for definite time from ~85 s to 125s, and finally disappeared after the evaporation finished. These temporally spectral evolutions confirmed that the capillary force from the ethanol evaporation induced the self-approaching of ZnO-Ag NRs hybrids to form the hot spots, making the Raman signals of 4-ATP well detected. Besides, a same volume droplet of other solvents such as acetone, methyl alcohol, isopropanol, ethyl acetate and ultrapure water were also added onto the dry ZnO-Ag NR hybrids, respectively (Figure S11-S15). The solvent

volatilization speed of acetone and methyl alcohol was much higher than that of ethanol. Therefore, the best scan-time was hard to be confirmed before the solvent volatilization process finished (Figure S11-12). There were much lower Raman signal of 4-ATP observed with the increase of observed time using isopropanol, ethyl acetate, and water as solvents due to the slow

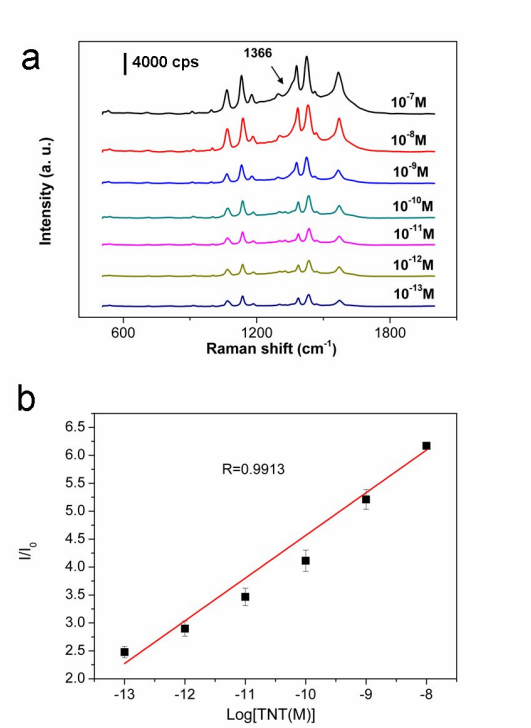

Figure 3 a) Raman responses of 4-ATP-functionalized ZnO-Ag hybrids with the presence of TNT at different concentrations: 1×10^{-7} to 1×10^{-13} M; b) The corresponding calibration curve for SERS intensity versus –log [TNT], in which the SERS intensities were recorded at 1430cm^{-1}.

volatilization rate (Figure S13-S15). In addition, the measurement of contact angle revealed a highly hydrophobic feature of the NR arrays for water (inset microscopic image of Figure S15). In contrast, other solvents could completely permeate into the interspaces of the ZnO-Ag NRs hybrids (inset of Figure S11-S14). Considering the factors of solvent evaporation rate and surface tension of different solvent, the collection time and the enhancement intensity of Raman peaks, ethanol was the most suitable solvents for formation capillarity-constructed reversible SERS hot spots during molecule detection.

Additionally, the stability of the ZnO-Ag NRs hybrid SERS substrates was evaluated. The lengths of 1.5 μm ZnO-Ag hybrids combining with ethanol as solvent were chosen. All R6G Raman spectra were obtained from 15 random points on the same piece of SERS substrate. The similar Raman spectra demonstrate the good signal reproducibility of this composite structure, and the relative standard deviation (RSD) of major R6G characteristic SERS peaks were calculated to evaluate the reproducibility of SERS signals. As shown in Figure S16, S17, it was revealing almost the same intensity for each characteristic band of R6G. The maximal RSD value of signal intensities of major SERS peaks was observed to be below 0.25, indicating that ZnO-Ag NRs hybrid SERS substrates had a good reproducibility across the entire area. The experimental results indicated that the flexible ZnO-Ag NRs could be used as highly sensitive, reproducible and reliable substrates for Raman practical applications.

Inspired by the huge SERS performance induced by the capillary force of solvent evaporation, the next goal was to explore the applications in practical molecule detection. When 1×10^{-13}M TNT alcoholic solution was added onto the 1.5 μm ZnO-Ag hybrids, it was surprising that the Raman signals of 4-ATP were violently enhanced (Figure 2b). The strongest signal intensity at 1430 cm^{-1} after ~45 s was ~3.55 times stronger than that obtained by the addition of pure ethanol (Figure 2c). It was because that the π-π conjugated structures between TNT and 4-ATP could effectively promote the electronic transfer, leading to the enhanced Raman signals by chemical mechanism (CM) enhancement (Figure S18-19).[18, 21] Similarly, the Raman signals of 4-ATP gradually disappeared with the evaporation of solvent finished. Based on the above results, the best measuring conditions for the detection of TNT were thus set at the volume of a 5 μL analyte droplet, data recorded at ~65 s after the addition of the liquid droplet, and the use of a 5 mW and 2 μm laser beam. Raman spectra of 4-ATP-functionalized ZnO-Ag hybrids with the presence of TNT at different concentrations were recorded (Figure 3a). The error bar line was shown in Figure 3b, the Raman intensity of PABT obviously increased with TNT concentrations from 100 fM to 0.1 μM and exhibited a correlation coefficient R = 0.9913 at the range of 100 fM to 10 pM. Even in the case of 40 fM TNT, the Raman signal of PABT was 1.26-fold stronger than that by the addition of blank ethanol, and thus a detection limit of 4×10^{-14} M TNT was reached (Figure S20-21).

Then, Raman spectra were obtained from TNT in the gas phase in the following manner.[22] The identical ZnO-Ag hybrid NR array SERS substrate was placed at the outlet of the pipe for 3 min where after a Raman spectrum was recorded. Then, a 5μL droplet of ethanol was added onto this hybrids SERS substrate, the clear enhancement of Raman spectra from a gradual increase to a gradual decrease were again observed, and the strongest signal intensity at 1430 cm^{-1} after ~45 s was ~7-times stronger than that from the pure 4-ATP Raman intensity in the same condition. The enhancement of 4-ATP Raman spectra was completely attributed to the contribution of ultratrace TNT, in solution or gas phase. After the substrate drying, we repeated adding ethanol for 4 times and recorded the Raman spectrum for 5 cycles. As shown in Figure 4, it was clear indicated that the ZnO-Ag NRs driven through the capillary force of solvent evaporation and formation highly SERS activity. Once the ZnO–Ag NRs hybrids substrate was enriched of TNT, just as been marked, this substrate could inform the existence of TNT even in 5 detection cycles through capillarity-constructed reversible hot spots approach. These measurements strongly demonstrated that 4-ATP-modified ZnO–Ag NRs hybrids could be used as a promising SERS platform for sensitive TNT detection.

On the platform of 4-ATP-modified ZnO-Ag NRs hybrids, the mechanism for TNT-induced resonance Raman enhancement of

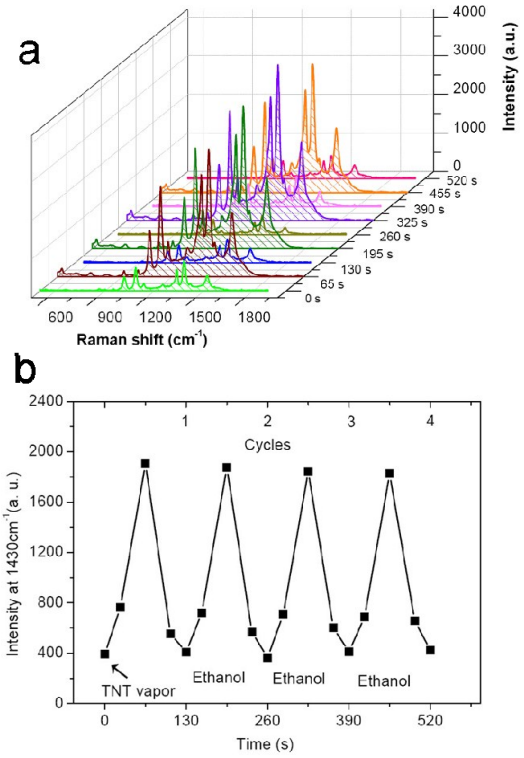

Figure 4 (a) Cyclic detection of 4-ATP Raman intensity at 1430 cm^{-1} after collection TNT vapor for 3 min, a 5μL droplet of pure ethanol was added onto this ZnO-Ag NRs hybrids SERS substrate before a Raman spectrum was recorded. Following the dryness of TNT ethanol, 5μL droplet of pure ethanol was added on the substrate and detected. (b) The temporal evolution of corresponding Raman intensity at 1430 cm^{-1} of (a).

4-ATP was proposed. As shown in Scheme 1, once the NR hybrids were exposed to ethanol, the ZnO NRs lean to form hot spots with the analyte molecules trapped between the top-closed NRs as the solvent evaporates from the arrays. The number of formed hot spots made it very likely that the TNT molecules would be located in a large number of hot spots giving rise to a large average Raman signal. Meanwhile, the π-π conjugated structures between TNT and 4-ATP could enhanced Raman signals by chemical mechanism (CM) enhancement (Figure S18-19).[18, 21] Thus the enhancement of the 4-ATP Raman signals mainly originated from the resonances of the molecular bridge with both incident laser and surface plasma, with the aid of Raman hot spots formed by the self-approaching of the long flexile NRs hybrids. To further ascertain the recognition selectivity of the 4-ATP-modified ZnO–Ag platform, we prepared other structurally similar nitrated-explosive detection systems (10^{-9} M in ethanol) such as picric acid (PA), 2-nitrotoluene (NT), and m-dinitrobenzene (DNB), and 2, 4-dinitrotoluene (DNT) (Figure 5 and Figure S22). It could be seen that compared with TNT, weaker Raman enhancements were observed for PA, DNT, DNB, and NT. In addition, the peak intensity at 1430 cm^{-1} was about 7.86 times stronger than that obtained without TNT (Figure 5a). However, other explosives were less than 2.5 times enhanced when acted with 4-ATP at the same condition. Moreover, the UV-vis spectrum did not show any visible absorption when DNB, DNT and PA was mixed with 4-ATP in solution, suggesting that DNB, DNT and PA could not likely form the effective charge-transfer complexing chromophore with 4-ATP (Figure 5b). All these experiments indicated that the 4-ATP-functionalized ZnO–Ag NRs hybrids provided an effective SERS platform for TNT detection with good sensitivity, reproducibility, and selectivity.

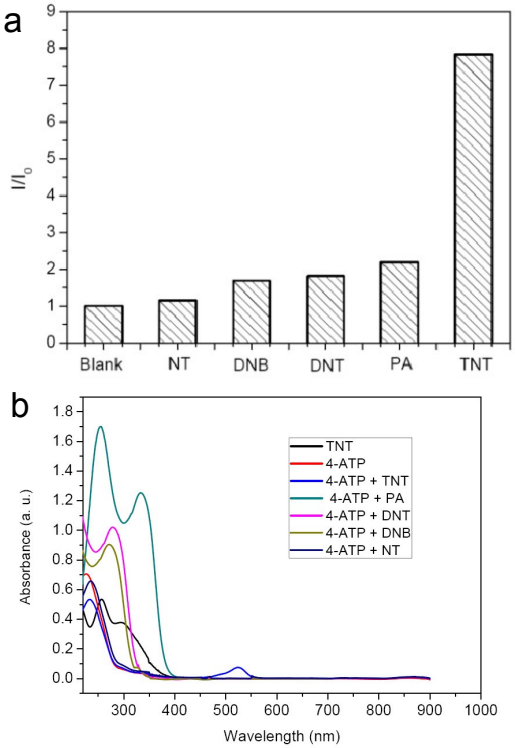

Figure 5. (a) Comparison of the SERS intensity (1430 cm^{-1}) of different explosives with the same concentration of 10^{-9} M in ethanol, (I was SERS intensity of 4-ATP interacted with explosives, and I_0 was SERS intensity of 4-ATP); (b) UV-vis absorption spectra of TNT, 4-ATP, TNT and 4-ATP complex, PA and 4-ATP complex, DNT and 4-ATP complex, DNB and 4-ATP complex, NT and 4-ATP complex. The UV-vis spectra in solution were obtained using ethanol with pH about 6.94 as the solvent at room temperature with a path-length of 1cm.

As we all known, Ag was recognized as one of the best surface enhanced Raman active material. However, the Ag-based nanomaterials would be easily oxidized gradually in air, as oxygen molecules could be absorbed onto the substrate surface and capture electrons from Ag atoms, leading to the oxidation of the surface Ag atoms to Ag+ ions. This would result in a loss of the hot spots and inactivation of the SERS substrate as a layer of silver oxide formed on the surfaces of these Ag nanomaterial (Scheme S1). And it was the most important reason why the Ag materials were limited in practical applications.[18] As a result, the reactivation of such an inactive substrate would be essential for practical SERS detection applications. Consequently, a hybrid substrate that was kept in dark air for a month was examined. It first yielded poor SERS signals (Figure 6a). However, when the substrate was irradiated with UV light, the ZnO NRs could

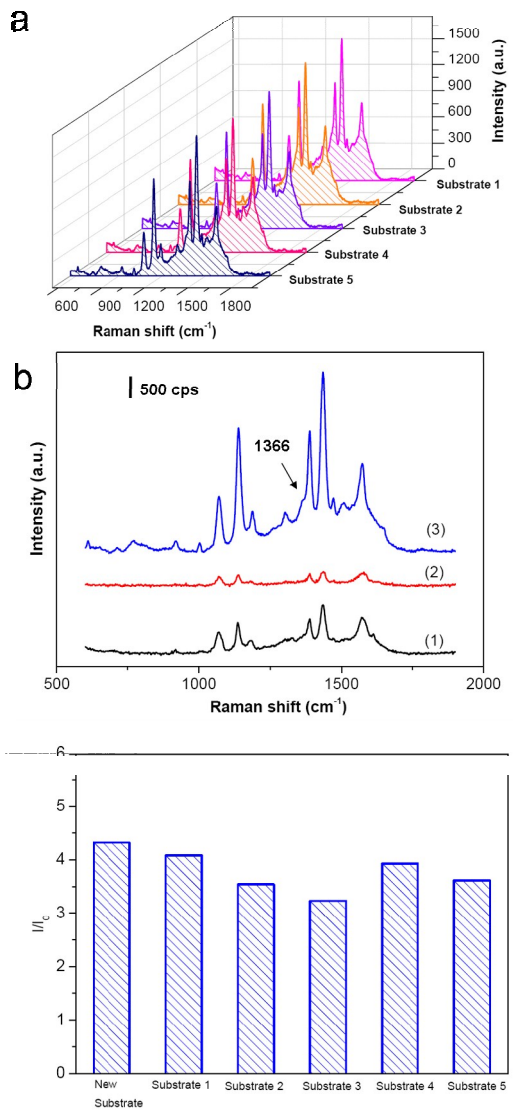

Figure 6 (a) SERS spectra of self-reviving substrates to detect TNT (1×10^{-12} M). The integration time is 5s; (b) curve (1) the as-prepared ZnO-Ag NRs hybrids substrate 1 of SERS spectra of probe 4-ATP; curve (2) kept substrate 1 in dark air for a month; curve (3) after irradiating with UV light for 5min for the substrate 1 in curve (2), then used this self-reviving substrate 1 to detect TNT (10^{-12} M) in ethanol. The integration time was 5s; (c) Comparison of the SERS intensity (1430 cm^{-1}) of five self-revive substrate and new as-prepared substrate with the same TNT detection condition of 10^{-12} M in ethanol. (I was SERS intensity of 4-ATP interacted with TNT, and I_0 was SERS intensity of 4-ATP).

absorb light in a particular region, and the excited electrons were eventually absorbed by the surface Ag+ ions, reducing the Ag+ ions to Ag atoms and reactivating the SERS inactive Ag-decorated ZnO substrate. It was clearly demonstrated that UV light irradiation could effectively and rapidly revive the hot spots of the SERS-inactive Ag-decorated ZnO substrate.[18] To evaluate the reproducibility of the self-reviving substrates, five substrates made from different batch were kept in dark air for a month, then revived under UV light and used as substrates to examine TNT (10^{-12} M) for comparison (Figure 6, Figure S23). The average deviation of peak height of the self-reviving substrates at 1430 cm^{-1} was 6.27%. In addition to the good self-revive reproducibility, five substrates displayed stable and high SERS enhancements in TNT detection. As shown in Figure S24, the distinct bands could be still easily identified in the Raman spectra even at the low concentration of 10^{-12} M by five self-revive substrates after 1 month. Moreover, the different self-reviving substrates were used for R6G, 4-ATP and TNT detection (Figure S23-S29). It should be noted that neither a shift in the major Raman peaks nor a significant change in Raman intensity occurred in SERS spectra from the substrate putted in dark cabinet for 30 days, revealing that the as-prepared substrate was stable for at least a 30-day period. This long-term stability in dark is of great importance for handling and storing the SERS-active substrates in practical applications.

Conclusion

In this paper, we reported for the first time the application of self-reviving SERS-active NR-shaped ZnO-Ag hybrids SERS substrates for the highly sensitive and selective detection of explosive TNT by the simple and efficient self-approaching strategy. During the detection, the self-approaching of the ZnO-Ag hybrids driven by the capillary force of solvent evaporation could efficiently and spontaneously induce the formation of reversible Raman hot spots. Different with other Ag-based SERS sensor, this SERS sensor could rapidly revive the hot spots of the SERS-inactive by simple UV light irradiation and keep stable SERS-active ability within 1 month. Furthermore, the SERS substrate could be employed for both liquid and gas phase TNT detection. The stable and ultrasensitivity SERS substrate demonstrates a new route to eliminate the oxidized inactive problem of traditional Ag-based SERS substrates and suggests promising applications of such hybrids as real-time online sensors for explosives detection. Further studies on the exploitation of other substrates for SERS applications are underway.

Acknowledgements

This work was supported by the National Natural Science Foundation (No. 21302176); China Postdoctoral Science Foundation (No. 2014M561843) and the Development Foundation of CAEP (No. 2013B0302042).

Notes and references

[a] *Institute of Chemical Materials, China Academy of Engineering Physics, Mianyang 621900, China;*
[b] *Key Laboratory of Materials Physics, Anhui, Key Laboratory of Nanomaterials and Nanostructures, Institute of Solid State Physics, Chinese Academy of Sciences, Hefei, 230031, China.*
**Address for correspondence. Email: xuan.hellen@gmail.com; sdlzb@issp.ac.cn; jackzhang531@gmail.com .*

† Electronic Supplementary Information (ESI) available: [details of any supplementary information available should be included here]. See DOI:10.1039/b000000x/

1. (a) R. S. Golightly, W. E. Doering, M. J. Natan, *ACS Nano* 2009, **3**, 2859-2869; (b) J. Homola, *Chem. Rev.* 2008, **108**, 462-493; (c) M. E. Stewart, C. R. Anderton, L. B. Thompson, J. Maria, S. K. Gray, J. A. Rogers, R. G. Nuzzo, *Chem. Rev.* 2008, **108**, 494-521.
2. (a) D. K. Lim, K. S. Jeon, H. M. Kim, J. M. Nam, Y. D. Suh, *Nat. Mater.*, 2010, **9**, 60-67; (b) A. Lee, G. F. S. Andrade, A. Ahmed, M. L. Souza, N. Coombs, E. Tumarkin, K. Liu, R. Gordon, A. G. Brolo, E. Kumacheva, *J. Am. Chem. Soc.,* 2011, **133**, 7563-7570; (c) M. Moskovits, *Nature*, 2010, **464**, 357-359.
3. (a) M. S. Schmidt, J. Hübner, A. Boisen, *Adv. Mater*, 2012, **24**, 11-18; (b) R. H. Que, M. W. Shao, S. J. Zhuo, C. Y. Wen, S. D. Wang, S. T. Lee, Adv. Funct. Mater. 2011, **21**, 3337-3343; (c) A. Kim, F. S. Ou, D. A. A. Ohlberg, M. Hu, R. S. Williams, Z. Y. Li, *J. Am. Chem. Soc.*, 2011, **133**, 8234-8235; (d) H. B. Tang, G. W. Meng, Q. Huang, Z. Zhang, Z. L. Huang, C. H. Zhu, *Adv. Funct. Mater.,* 2012**, 22**, 218-224.
4. (a) Y. Fang, N. H. Seong, D. D. Dlott, *Science* 2008, **321**, 388-392; (b) N. P. W. Pieczonka, R. F. Aroca, *Chem. Soc. Rev.* 2008**, 37**, 946-954; (c) D. K. Lim, K. S. Jeon, H. M. Kim, J. M. Nam, Y. D. Suh, *Nat. Mater.* 2010, **9**, 60-67; (d) S. Z. Li, M. L. Pedano, S. H. Chang, C. A. Mirkin, G. C. Schatz, *Nano Lett.* 2010, **5**, 1722-1727; (e) L. Polavarapu, L. M. Liz-Marz´an, *Phys. Chem. Chem. Phys.,* 2013, **15**, 5288-5294; (f) L. B. Yang, P. Li, H. L. Liu, X. H. Tang, J. H. Liu, *Chem. Soc. Rev.,* 2015, DOI: 10.1039/C4CS00509K.
5. W. Dickson, G. A. Wurtz, P. R. Evans, R. J. Pollard, A. V. Zayats, *Nano Lett.*, 2008, **8**, 281-287.
6. H. L. Chen, K. C. Hsieh, C. H. Lin, S. H. Chen, *Nanotechnology*, 2008, **19**, 435304-435309.
7. (a) G. Xu, Y. Chen, M. Tazawa, P. Jin, *J. Phys. Chem. B,* 2006, **110**, 2051-2058; (b) G. Xu, C. M. Huang, M. Tazawa, P. Jin, D. M. Chen, *J. Appl. Phys.,* 2008, **104**, 053102-053110.
8. (a) S. Olcum, A. Kocabas, G. Ertas, A. Atalar and A. Aydinli, *Opt. Express,* 2009, **17**, 8542-8546; (b) K. D. Alexander, K. Skinner, S. Zhang, H. Wei, R. Lopez, *Nano Lett.,* 2010, **10**, 4488-4494.
9. (a) H. B. Zhou, Z. P. Zhang, C. L. Jiang, G. J. Guan, K. Zhang, Q. S. Mei, R. Y. Liu, S. H. Wang, *Anal. Chem.* 2011, **83**, 6913-6917; (b) H. L. Liu, Y. D. Sun, Z. Jin, L. B. Yang, J. H. Liu, *Chem. Sci.*, 2013, **4**, 3490-3496.
10. (a) M. Cerruti, J. Jaworski, D. Raorane, C. Zueger, J. Varadarajan, C. Carraro, S. W. Lee, R. Maboudian, A. Majumdar, *Anal. Chem,* 2009, **81**, 4192-4199; (b) M. Riskin, R. T. Vered, T. Bourenko, E. Granot, I. Willner, *J. Am. Chem. Soc.*, 2005, **127**, 6744-6751.
11. (a) A. G. Dong, J. Chen, P. M. Vora, J. M. Kikkawa, C. B. Murray, *Nature* 2010, **466**, 474-477; (c) A. M. Smith, S. M. Nie, *Acc. Chem. Res.* 2010, **43**, 190-200; (d) X. G. Peng, *Acc. Chem. Res.* 2010, **43**, 1387-1395.
12. (a) K. A. Willets, R. P. Van Duyne, *Annu. Rev. Phys. Chem.*, 2007, **58**, 267-297; (b) J. Kneipp, H. Kneipp, K. Kneipp, *Chem. Soc. Rev.*, 2008, **37**, 1052-1060.
13. R. S. Golightly, W. E. Doering, M. J. Natan, *J. Am. Chem. Soc. Nano,* 2009, **3**, 2859-2869.
14. W. Y. Li, P. H. C. Camargo, X. M. Lu, Y. N. Xia, *Nano Lett.* 2009, **9**, 485-490; (b) B. H. Zhang, H. S. Wang, L. H. Lu, K. L. Ai, G. Zhang, X. L. Cheng, *Adv. Funct. Mater.* 2008, **18**, 2348-2355.
15. (a) H. B. Zhou, Z. P. Zhang, C. L. Jiang, G. J. Guan, K. Zhang, Q. S. Mei, R. Y. Liu, S. H. Wang, *Anal. Chem.* 2011, **83**, 6913-6917; (b) H. L. Liu, Y. D. Sun, Z. Jin, L. B. Yang, J. H. Liu, *Chem. Sci.*, 2013, **4**, 3490-3496; (c) L. B. Yang, H. L. Liu, J. Wang, F. Zhou, Z. Q. Tian, J. H. Liu, *Chem. Commun.*, 2011, **47**, 3583-3585; (d) K. Qian, L. B. Yang, Z. Y. Li, J. H. Liu, *J. Raman Spectrosc.* 2013, **44**, 21-28.
16. (a) P. Taladriz-Blanco, N. J. Buurma, L. Rodriguez-Lorenzo, J. Perez-Juste, L. M. Liz-Marzan, P. Herves, *J. Mater. Chem.,* 2011, **21**, 16880-16887; (b) T. Demeritte, R. Kanchanapally, Z. Fan, A. K. Singh, D. Senapati, M. Dubey, E. Zakarb, P. C. Ray, *Analyst*, 2012, **137**, 5041-5045.
17. (a) M. S. Goh, M. Pumera, *Anal. Bioanal. Chem.*, 2011, **399**, 127-131; (b) S. W. Thomas III, G. D. Joly, T. M. Swager, *Chem. Rev.,* 2007, **107**, 1339-1386; (c) M. Riskin, R. Tel-Vered, O. Lioubashevski, I. Willner, *J. Am. Chem. Soc.,* 2009, **131,** 7368-7378; (d) C. J. McHugh, A. R. Kennedy, W. E. Smith, D. Graham, *Analyst*, 2007, **132**, 986-988.
18. (a) M. M. Liu, W. Chen, *Biosensors and Bioelectronics,* 2013, **46**, 68-73; (b) X. He, H. Wang, Z. B. Li, D. Chen, Q. Zhang, *Phys. Chem. Chem. Phys.,* 2014, **16**, 14706-14712; (c) H. L. Liu, D. Y. Lin, Y. D. Sun, L. B. Yang, J. H. Liu, *Chem. Eur. J.* 2013*,* **19**, 8789-8796; (d) X. Zhou, H. L. Liu, L. B. Yang, J. H. Liu, *Analyst*, 2013, **138**, 1858-1864.
19. X. M. Zhao, B. H. Zhang, K. L. Ai, G. Zhang, L. Y. Cao, X. J. Liu, H. M. Sun, H. S. Wang, L. H. Lu, *J. Mater. Chem.,* 2009, **19**, 5547-5553.
20. C. Ruan, G. Eres, W. Wang, Z. Zhang, B. Gu, *Langmuir*, 2007, **23**, 5757-5759.
21. (a) L. B. Yang, L. A. Ma, G. Y. Chen, J. H. Liu, Z. Q. Tian, *Chem. Eur. J.*, 2010, **16**, 12683-12693; (c) Y. R. Fang, Y. Z. Li, H. X. Xu, M. T. Sun, *Langmuir*, 2010, **26**, 7737-7746. (d) K. A. Mahmoud, M. Zourob, *Analyst*, 2013, **138**, 2712-2719.
22. A saturated solution of TNT in ethanol was made. 1 ml of TNT solution was deposited onto wad of wool, which was inserted into a long copper pipe with 100mL volume. The pipe was inserted into the heater, which contained 60 °C such that the two ends of the pipe protruded. Through fixtures nitrogen carrier gas was blown through the heated pipe. The nitrogen gas at the exit of the heated pipe was assumed to be saturated with TNT.